Conduction-electron spin resonance in small particles of sodium*

Daniel A. Gordon†
Physics Department, University of California, Berkeley, California 94720
(Received 4 November 1975)

Results of conduction-electron spin-resonance (CESR) measurements on small sodium particles formed in x-irradiated sodium azide are interpreted according to a simple model which includes the effects of a broad particle size distribution and the presence of surface spins. Estimates of line broadening due to exchange interaction between the surface spins and the conduction electrons are found to be consistent with experimentally observed broadening at helium temperatures. A signal observed at the sodium CESR g value for very low incident microwave power level is considered to represent a hyperfine envelope of CESR signals from particles exhibiting quenched spin-lattice relaxation resulting from discreteness of the conduction-electron energy levels.

I. INTRODUCTION

Observation of conduction-electron spin resonance (CESR) has been reported in a relatively small number of metals. Using standard reflection techniques, CESR has been seen in "bulk" metals of Li, Na, K, Rb, Cs, Be, Mg, Al, and Ca.[1] Using the selective transmission method, CESR has been seen in bulk samples of Li, Na, K, Rb, Cs, Mg, Al, Cu, Ag, and Au.[2] Bulk samples refers to samples large enough in dimension so that the conduction-electron energy levels are quasi-continuous.

In the heavier metals the conduction-electron spin relaxation times are extremely short, giving rise to very broad CESR lines which have been difficult or impossible to detect. However, it was suggested by Kubo[3] and Holland[4] that in sufficiently small metal particles the usual relaxation mechanisms should be quenched due to discreteness of the conduction-electron energy levels, leading to narrowed CESR lines. In a theoretical treatment of CESR in small particles Kawabata[5] has given two criteria for narrowing due to level discreteness:

$$\hbar\omega_z/\Delta \ll 1, \tag{1}$$

$$\hbar/\tau\Delta \ll 1, \tag{2}$$

where τ is given by $d/v_F(\Delta g)^2$, d is the particle diameter, v_F is the Fermi velocity, Δ is the mean energy-level spacing, ω_z is the Zeeman frequency, and Δg is the g shift. For usual microwave frequencies, particles in the size range below 100 Å are required for Kawabata's criteria to hold. Observations of CESR signals from particles in this size range have been reported for Li,[6] Na,[7] K,[8] Al,[9] Ag,[10] Au,[11] and Pt,[12] and claims of narrowing of the CESR lines due to level separation have been made for all of these except Na and K.

In addition to level separation effects, the interpretation of small-particle CESR data is complicated by such effects as particle size distributions, surface interactions, nuclear hyperfine broadening, and the presence of impurity resonances which may obscure, or be mistaken for, CESR signals. To distinguish among these effects it is desirable to obtain data for a wide range of particle sizes, from bulk down to a few tens of angstroms. Such a study was carried out for Li particles in neutron-irradiated LiF.[13] In view of the extremely small spin-orbit coupling in Li it is of interest to investigate CESR in small particles of a heavier metal, but one in which CESR can still be observed readily in bulk, such as sodium.

In this paper is presented a simple self-consistent interpretation of data from a CESR study of small sodium particles formed in x-irradiated sodium azide (NaN_3). In such samples the particle size can be varied from a few tens of angstroms to several microns by controlling the annealing time and temperature. In a similar study, Smithard[14] found unexplained broadening at 4.2 K in some samples but no quantum level separation effects. Since an understanding of CESR in small particles of a relatively free-electron-like well-studied metal such as sodium should be of great value in interpreting CESR data for other metals, the questions left unanswered by Smithard merit further investigation. In particular, the sources of low-temperature broadening and the unexplained failure to observe a level separation effect are of interest. In the present work, we have observed unusual line shapes; low-temperature broadening; and, at very low power levels, a signal with long T_1. We explain these data on the basis of particle size distributions; interactions between conduction electrons and surface spins; and, in the smallest particles, increased conduction-electron relaxation times due to level discreteness, together with inhomogeneous broadening from nuclear contact hyperfine interactions.

II. THEORETICAL BACKGROUND

A. CESR in bulk particles

In particles smaller than the rf skin depth but too large to exhibit level separation effects, the expected CESR line shape is Lorentzian, and the derivative peak-to-peak linewidth is determined by the spin-lattice relaxation time T_{sl} according to the relation

$$\Delta H_{pp} = 2/\sqrt{3}\,\gamma_s T_{sl}, \tag{3}$$

where γ_s is the conduction electron gyromagnetic ratio.

1. Conduction-electron spin relaxation

The principal mechanisms contributing to the spin-lattice relaxation are usually spin-flip scattering by phonons, by nonmagnetic impurities and by surfaces:

$$1/T_{sl} = (1/T_1)_{ph} + (1/T_1)_i + (1/T_1)_s. \tag{4}$$

The surface scattering term $(1/T_1)_s$ is of special importance for small particles. It may be assumed that a conduction electron will have its spin flipped in a fraction ϵ of its collisions with the surface, leading to an equation of the form

$$(1/T_1)_s = 3\epsilon v_F/d \tag{5}$$

for a spherical particle of diameter d.[15]

Recent calculations[16,17] indicate that spin-orbit scattering at ideal surfaces cannot account for the experimentally observed values of ϵ, but agreement can be obtained assuming a spin flip mechanism involving an exchange interaction with magnetic centers on the surfaces. According to an argument of Walker,[18] Eq. (5) is valid provided $d \ll \delta_s = [(\frac{1}{3}v_F\lambda)T_{sl}]^{1/2}$ where λ is the electron mean free path. The spin diffusion length δ_s is about 10 μm for sodium at room temperature.

2. Line broadening due to spins in the matrix

Consider an idealized sample consisting of spherical particles of diameter d embedded in a dielectric matrix containing spins S. Some of the spins may be close enough to particle surfaces to interact with the conduction electrons via an exchange interaction. Others will influence the CESR only by the contribution of their dipole fields to the local fields experienced by the conduction electrons.

a. *Exchange effects.* For a system of conduction electrons interacting via exchange with a small concentration of localized spins, ESR can be described by coupled Bloch equations.[19] Such coupled equations are usually applied to dilute magnetic alloys such as Cu:Cr.[20] Although local moments have not been reported in sodium, we may apply the coupled Bloch equations to the case of a sample of small sodium particles each having a small number of surface spins exchange coupled to the conduction electrons.

The Hamiltonian for the interaction between the ith conduction electron and the jth surface spin is $\mathcal{H}_{ex} = -2J\delta(\vec{r}_i - \vec{R}_j)\vec{s}_i \cdot \vec{S}_j$, where $\vec{r}_i$ is the position of the ith conduction electron, with spin operator $\vec{s}_i$; $\vec{R}_j$ is a lattice site in the surface associated with the jth surface spin, having spin operator $\vec{S}_j$; and J is the exchange integral, which in this case takes account of the fact that the interaction may be much reduced from the case of a local moment located at an interior lattice site because the surface spin may be located not at $\vec{R}_j$, but rather just outside the surface at a position adjacent to $\vec{R}_j$.

If the exchange coupling is sufficiently strong, the solution of the coupled Bloch equations corresponds to a single coupled-mode resonance with an effective T_1 given by[20]

$$\left(\frac{1}{T_1}\right)_{eff} = \frac{1}{T_{sl}}\left(\frac{1}{1+\chi_r}\right) + \frac{1}{T_{ml}}\left(\frac{\chi_r}{1+\chi_r}\right), \tag{6}$$

where s and m refer to the conduction electron and surface spin systems, respectively, $\chi_r = \chi_m^0/\chi_s^0$ is the ratio of the static susceptibilities of the two spin systems, and T_{ml} is a spin-lattice relaxation time for the surface spins. It may be necessary for the localized spins to be incorporated into the metal surface layer for this strong-coupling limit to apply. Note that since the conduction-electron and local moment spin systems approach a common spin temperature in the strong-coupling limit, the exchange spin-flip scattering mechanism proposed to account for the magnitude of the surface spin-flip scattering parameter ϵ[16,17] would not lead to relaxation of the conduction-electron spins.

If the exchange coupling is sufficiently weak so that cross relaxation between the spin systems is negligible, the conduction-electron resonance will be shifted due to the effective exchange field $\lambda\vec{M}_m^0$, where λ is a molecular-field constant and $\vec{M}_m^0$ is the surface spin equilibrium magnetization. The shift is

$$\Delta H = \lambda\chi_m^0 H_0 = 2JcSB_S/\gamma_s\hbar \tag{7}$$

where c is the equivalent volume concentration of surface spins, B_S is the Brillouin function with argument $g_m S\mu_B H_0/kT$, and J is related to λ by $\lambda = 2J\Omega/\gamma_s\gamma_m\hbar^2$ with Ω an atomic volume. This shift can lead to inhomogeneous broadening of the CESR because of (i) a distribution of positive and negative values of J among surface spin sites, and (ii) a statistical distribution in the net number of unpaired surface spins among particles if the surface spins are flipping slowly compared to $1/T_{sl}$.

The distribution in J leads to a broadening of magnitude given by Eq. (7) with J replaced by an average magnitude $|J|_{av}$. Let n be the number of surface spins per particle. For given J and n, the statistical distribution in the case of slowly flipping local moments leads, by a random walk argument, to an inhomogeneous broadening of magnitude

$$\Delta H \sim 2JcS/n^{1/2}\gamma_s\hbar \tag{8}$$

which is independent of temperature, and which exceeds the broadening given by (7) only for very small n.

b. *Local moment dipole fields*. Owing to its rapid motion, a conduction electron in a small particle senses the average over the particle volume of the dipole magnetic field of a localized spin in the matrix. The component of this average dipole magnetic field in the direction of the applied static field gives a shift of the conduction-electron resonance. This shift may be positive or negative, depending on the orientation of the local moment and on its position. By a random-walk argument, therefore, the inhomogeneous broadening due to n such spins would be of order $n^{1/2}\delta H$, where δH is the magnitude of the shift due to a single spin. If the localized spins are flipping slowly compared with the conduction-electron relaxation rate, the broadening is roughly

$$\Delta H \sim n^{1/2}\gamma_m\hbar S/(\tfrac{1}{2}d)^3 \tag{9}$$

whereas if the localized spins are flipping rapidly it is

$$\Delta H \sim n^{1/2}\gamma_m\hbar S B_S/(\tfrac{1}{2}d)^3 \tag{10}$$

B. CESR in very small particles in the quantum level separation regime

When both of Kawabata's criteria, Eqs. (1) and (2), are satisfied, the CESR signal comes from the particles with an odd number of conduction electrons and consists of a collection of very sharp lines with a distribution of g shifts corresponding to the variety of level structures of the particles. Thus, the CESR is inhomogeneously broadened and has a very long T_1. Kawabata's[5] results for the CESR linewidth versus particle diameter are plotted for sodium in Fig. 1. Kawabata also predicts a shift, of the same magnitude as the linewidth, to higher field. Of particular interest is the d^2 dependence of the linewidth for diameters below about 100 Å. Also plotted in Fig. 1 are some published data points of Smithard[14] for colloidal sodium particles in x-irradiated NaN_3 samples. A temperature-dependent linewidth of $0.023T$ G (see Sec. V) has been subtracted from Smithard's linewidths for comparison with Kawabata's theory.

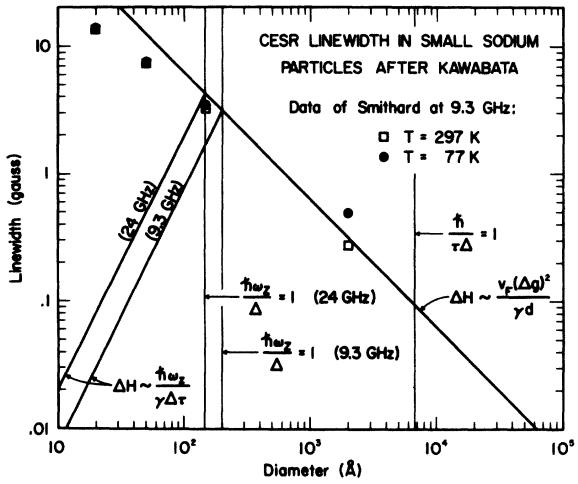

FIG. 1. CESR linewidth vs particle diameter for small solium particles at X and K bands, after Kawabata (see Ref. 5). The linewidth is $\Delta H \sim \hbar\omega_z/\gamma\Delta\tau$ for $\hbar/\tau\Delta, \hbar\omega_z/\Delta \ll 1$, and $\Delta H \sim v_F(\Delta g)^2/\gamma d$ for $\hbar\omega_z/\Delta \gg 1$, $\hbar/\tau\Delta \ll 1$ and for $\hbar\omega_z/\Delta, \hbar/\tau\Delta \gg 1$. Also shown are data points of Smithard (see Ref. 14, Fig. 4) with the temperature-dependent term $\Delta H_{ph} = .023T$ G subtracted out.

Smithard found no evidence of the d^2 dependence for small diameters.

Linewidth contributions from phonon and surface spin-orbit spin-flip scattering are expected to be quenched due to quantum level separation. However, other broadening mechanisms, absent in Kawabata's treatment, should be considered in interpreting experimental data. Such mechanisms include broadening due to surface spins and broadening due a distribution of nuclear hyperfine fields.

The nuclear contact hyperfine broadening can be expected to be important for sub-100-Å particles of sodium, assuming that the average s-character conduction-electron density at a sodium nucleus remains approximately equal to its bulk value. Consider a conduction electron which interacts with N equivalent nuclei of spin I. The resonance field for CESR becomes

$$H_R = \frac{\omega_g}{\gamma_s} - \sum_{i=1}^{N} I_i^z h_{hf}, \tag{11}$$

where h_{hf} is an effective contact hyperfine field, and I_i^z is the z-component spin operator for the ith nucleus. For atomic sodium, the contact hyperfine coupling is 316 G,[21] but this value is reduced for metallic sodium by a factor ξ, equal to 0.60,[22] giving $h_{hf} = 190/N$. The resulting nearly Gaussian envelope of hyperfine lines has a peak-to-peak derivative linewidth $\Delta H_{pp} = 423/N^{1/2}$ G. The number of atoms in a spherical particle of diameter d with bcc structure is $N = \frac{4}{3}\pi(\frac{1}{2}d)^3/(\frac{1}{2}a_0^3)$, where the lattice constant a_0 is 4.225 Å at 5 K for sodium.[23] (For a

particle only a few lattice constants across, this relation may be considered to define the diameter in terms of the number of atoms.) The hyperfine broadening for spherical sodium particles is then

$$\Delta H_{pp} = 3600/d^{3/2}\ \text{G}, \tag{12}$$

where d is in angstroms. For $d = 100$ Å this gives $\Delta H_{pp} = 3.6$ G.

III. EXPERIMENTAL METHODS

Measurements were made on both powder and single-crystal samples of x-irradiated NaN_3.

The powder samples consisted of nominally 98% pure NaN_3 powder. No effort was made to purify them, and spectrographic analysis indicated the presence of 0.17-at.% calcium, 0.003-at.% magnesium, and 0.002-at.% iron.

The single crystals were grown by the method of precipitant infusion using acetone as the precipitant. They grew as flat plates with the c axis perpendicular to the broad faces, and were typically 0.5 mm thick and up to 1 cm across after eight weeks of growth. The starting material for the single-crystal samples was nominally 99% pure NaN_3 purified by multiple reprecipitation. Spectrographic analysis of a single crystal for various metal impurities indicated the presence of 0.0006-at.% calcium and 0.0007-at.% manganese.

Most samples were irradiated in evacuated quartz or Pyrex tubes with x-rays produced by bombarding a large tungsten or tantalum plate with 8-MeV electrons from a linear electron accelerator. (Exceptions will be noted.) High-energy x rays were employed in order to achieve uniform coloring of large samples. The irradiation dose was estimated using a calibrated cobalt-glass dosimeter, and was typically on the order of 10 Mrad. Nominal sample temperature during irradiation was room temperature, but some samples showed evidence of heating in the x-ray beam.

Annealing of the samples was necessary to produce a concentration of sodium detectable by ESR. Small samples were annealed in a Varian E-4540 variable temperature controller; large samples were annealed in a temperature regulated oven. Samples were annealed in evacuated sample tubes unless otherwise noted.

ESR measurements were carried out at 9.5 and 24 GHz. The 9.5 GHz spectrometer was a Varian Model E-3, with 100-kHz field modulation. A Varian E-4540 variable temperature controller maintained sample temperatures in the range −160°–300°C. Measurements at 24 GHz were made with a superheterodyne spectrometer using 300-Hz field modulation.

IV. CHARACTERIZATION OF SAMPLES

The samples generally turned uniformly yellow on irradiation, and darkened on annealing at temperatures between about 180° and 300°C, appearing black after a few minutes.

With continued heating in air at temperatures above about 250°C, powder samples became dark blue-violet. When such a blue-violet sample was left standing in air the color slowly faded to white; x-ray diffraction from a partially faded sample indicated the presence of $Na_2CO_3 \cdot H_2O$.

The effect of annealing on single-crystal samples was similar to that for powder samples. In addition, the following features were noted:

(i) After turning black, the crystals fragmented into powder when the concentration of Na metal as determined by CESR reached a few tenths of one percent.

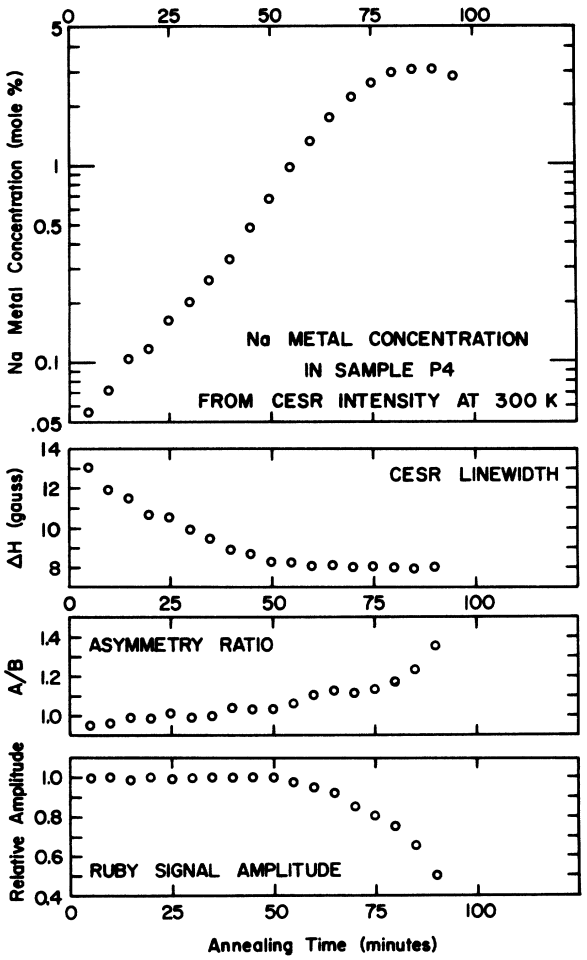

FIG. 2. Room-temperature CESR integrated intensity, linewidth, and asymmetry ratio as a function of isochronal annealing at 250 °C for sample $P4$. Also shown is the relative amplitude of the ruby intensity standard signal.

(ii) When an intact black crystal was crushed, the fragments were observed to be red or red-purple in transmission.

(iii) Although all crystals appeared to be uniformly yellow after irradiation, some of them showed a layer effect after annealing. Such crystals were deeply colored near the surfaces but had colorless interiors.

The concentration of metallic sodium in a sample was determined from the ratio of the integrated intensity of the CESR signal to that of a calibrated ruby or phosphorus-doped-silicon intensity standard signal. The sodium concentration was found to increase approximately exponentially in time from first observation until it reached a value on the order of 1 mole% during annealing of samples at 250°C in vacuum. Figure 2 shows the results of CESR measurements at 300 K as a function of isochronal annealing of a powder sample at 250°C. The measured quantities are the Na metal concentration, peak-to-peak derivative linewidth and asymmetry ratio as well as the amplitude of the ruby intensity standard signal which gives a relative measure of the cavity Q. As observed by Smithard,[14] the CESR linewidth decreased with annealing. This behavior is attributed to decreasing of $(1/T)_s$ with increasing particle size. After about 50 min the CESR signal began to show asymmetry, indicating particle dimensions comparable with the microwave skin depth of about 1 μm, and the total volume of sodium metal became sufficiently large to lower noticeably the cavity Q. The final value of the linewidth at 300 K was 8 G, whereas the value for pure bulk sodium is between 6 and 7 G.[24] This discrepancy is thought to be due to a wide distribution of particle sizes resulting from nonuniform annealing of this sample rather than to impurities in the particles. Other samples, annealed in the large oven, attained a room-temperature linewidth of 7 G without displaying asymmetry.

In addition to CESR, several other EPR signals were observed. A strong resonance previously identified as due to the N_2^- molecule ion at an azide vacancy[25] was detected in all the irradiated samples which were studied by ESR at 4.2 K before annealing. Annealing decreased the intensity of the N_2^- resonance, but only in a very heavily annealed blue-violet powder was it no longer detectable. After light annealing some single-crystal samples displayed another EPR signal at approximately $g = 2.0035$; this resonance was characterized by a nearly isotropic g value and anisotropic hyperfine structure. (A similar resonance was reported by Smithard for one crystal orientation.[14]) At 4.2 K superhyperfine structure was resolved. Identification of this resonance will be the subject of a future publication. Several additional weaker unidentified EPR signals were observed, particularly in unannealed or lightly annealed samples.

Attempts were made to determine the sodium concentration and the particle size distribution in some single-crystal samples by x-ray diffraction line broadening, NMR, and electron microscopy of cleavage surface replicas, but without success. The sodium metal concentration was insufficient, and the cleavage surfaces of darkened crystals appeared to be unstable and unsuitable for replication. Estimations of particle size were therefore based on the optical and ESR measurements of Smithard,[14] as described in Sec. V.

V. RESULTS AND DISCUSSION

A. Size distribution and surface effects for bulk particles

Figure 3 shows the CESR linewidth vs temperature for powder samples $P1$, $P2$, and $P3$ which are at different stages of particle growth. These samples were irradiated and annealed in air. The line shapes were approximately Lorentzian.

From Eqs. (3)–(5) and Yafet's[26] calculation of the temperature dependence of $(1/T_1)_{ph}$ the linewidth between 77 and 300 K has the form

$$\Delta H_{pp} = \Delta H_{ph} + \Delta H_i + \Delta H_s = AT + \Delta H_i + B/d. \quad (13)$$

The impurity term ΔH_i can be neglected since particles formed in NaN_3 by x-irradiation and annealing should be quite pure. For sample $P1$ this was verified by the fact that the CESR linewidth at 4.2 K was only 0.3 G.

From Na CESR linewidth measurements reported in the literature, an average value of A is 0.023 ±0.004 G/K. For the data of Fig. 3, A is 0.022 G/K. The constant B may be estimated from the data of Smithard.[14] Again neglecting ΔH_i, we have (see Fig. 1) $B \approx 260$ G-Å. The resulting approxi-

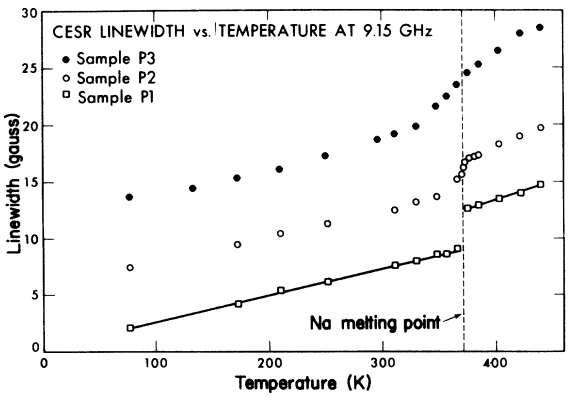

FIG. 3. CESR linewidth versus temperature at 9.15 GHz for samples P1, P2, and P3.

mate expression for the linewidth is

$$\Delta H_{pp} = 0.023T + 260/d, \quad (14)$$

with d in angstroms. From Eq. (14) and Fig. 3, the particles in samples $P3$, $P2$, and $P1$ have mean diameters 24, 52, and 1350 Å, respectively.[27]

Linewidth measurements at 4.2 K for samples $P3$ and $P2$ were not possible because the CESR signals were obscured by intense N_2^- powder pattern resonances.

Figures 4(a)–4(c) and 5(a) show the CESR line shapes at moderate microwave power level for single-crystal sample $SC1$ at 297, 195, 77, and 4.2 K, compared with Lorentzian line shapes of the same peak-to-peak amplitude and width. As the temperature is reduced the wings of the CESR lines grow with respect to the Lorentzian curves. The linewidth is plotted against temperature in Fig. 6 for samples $SC1$ and $P1$. Between 77 and 300 K the slope of the data for sample $SC1$ is

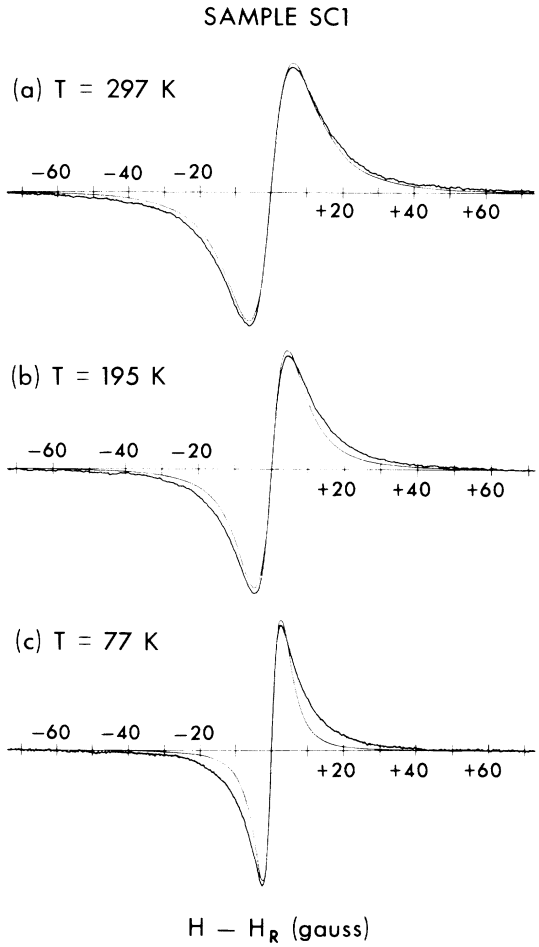

FIG. 4. CESR line shapes at 24 GHz in sample SC1 at (a) 297 K, (b) 195 K, and (c) 77 K. On each trace is superimposed a Lorentzian derivative curve having the same peak-to-peak amplitude and linewidth as the data. The slight asymmetry in the data is probably due to an admixture of dispersion signal.

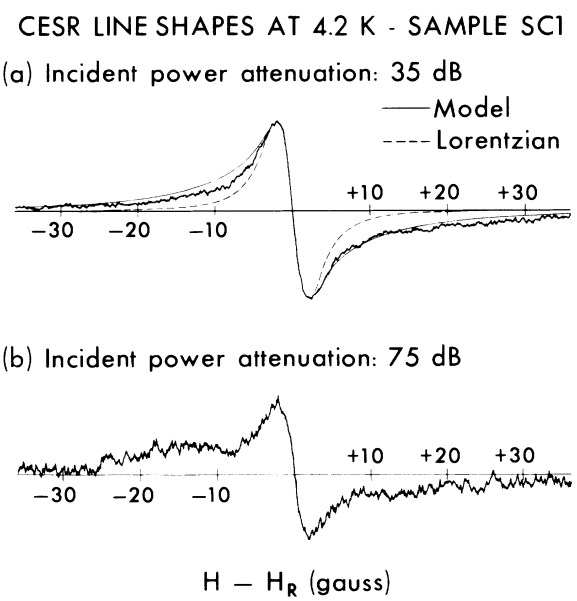

FIG. 5. CESR line shapes at 24 GHz in sample SC1 at 4.2 K. Part (a) shows a trace obtained at a moderate microwave power level, together with the MSD superposition line shape (solid line) and a Lorentzian derivative curve having the same peak-to-peak amplitude and linewidth as the data (dashed line). Part (b) shows a trace obtained at greatly reduced microwave power.

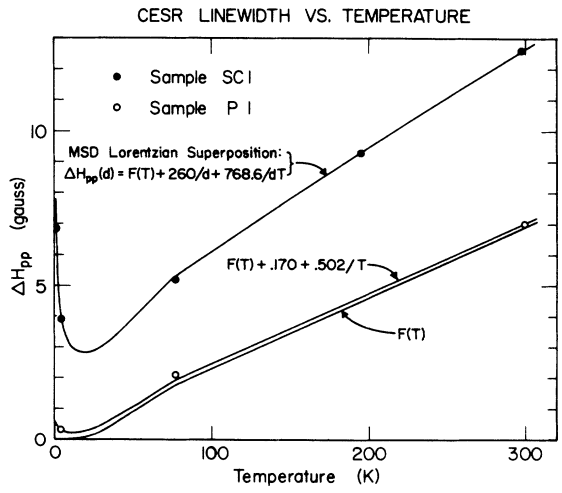

FIG. 6. CESR linewidth versus temperature, showing data points for samples $SC1$ and P1 at 24 GHz. The solid line through the data points for sample $SC1$ is calculated for the MSD composite line shape. The solid line through the data points for sample $P1$ represents Eq. (15) with $d = 1350$ Å. The function $F(T)$, defined in the text, is also plotted.

0.035 G/K, in apparent disagreement with Eq. (14).

Both the enhancement of the wings and the increased slope can be accounted for by assuming an appropriate broad particle size distribution for sample $SC1$. (Evidence of inhomogeneous particle growth is not unexpected for this sample, since it was one of the crystals displaying layered coloration, as described in Sec. IV.) Such a distribution is $P(d) \propto d^{-5}$ between limiting diameters $d_{\min} = 12$ Å and $d_{\max} = 195$ Å. For this size distribution, which we shall refer to as the model size distribution or MSD, the relative weighting of large and small particles is such that the linewidth of the composite resonance has a steeper temperature dependence than the linewidth for a single particle size. The values of $d_{\min}$ and $d_{\max}$ in the MSD were chosen to give agreement between the linewidth of the MSD composite resonance and the data for sample $SC1$ at 77 and 297 K. Agreement at 195 K followed. The MSD composite line shapes are compared with the data in Fig. 7. The size distribution leads to enhancement of the wings of the resonance with decreasing temperature; the agreement with the data is particularly good at 77 K.

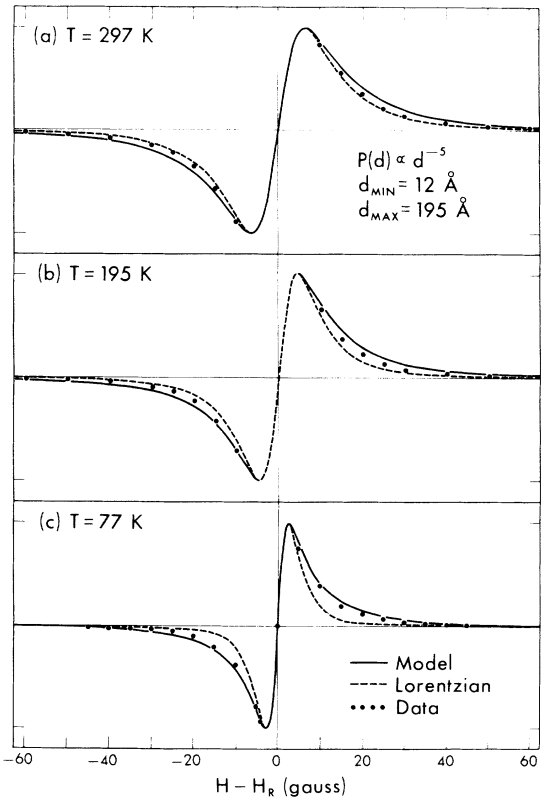

FIG. 7. Comparison of MSD composite line shapes for sample $SC1$ (solid lines) with the data and Lorentzian curves of Fig. 4 at (a) 297 K, (b) 195 K, and (c) 77 K.

Using the MSD for sample $SC1$ and assuming a single particle size for sample $P1$, the linewidth data for these samples can be accounted for over the entire temperature range in Fig. 6 by modifying Eq. (14) to read[27]

$$\Delta H_{pp} = F(T) + 260/d + 768.6/dT \qquad (15)$$

with d in angstroms, where $F(T)$ is the phonon term, approximated here as

$$F(T) = \begin{cases} 0.023T, & T \geq 77 \text{ K} \\ 2/\sqrt{3}\,\gamma_s T_s, & T \leq 77 \text{ K} \end{cases}$$

and T_s is the spin relaxation time from the theory of Yafet[26] as evaluated by Kolbe,[28] slightly renormalized to make $F(T)$ continuous. The third term on the right in Eq. (15) represents low-temperature broadening. In Fig. 6 the solid lines represent $F(T)$, the linewidth of Eq. (15) for $d = 1350$ Å, and the linewidth obtained from a superposition of Lorentzians of width given by Eq. (15) weighted according to the MSD. The line shape at 4.2 K calculated using Eq. (15) and the MSD is in good agreement with the data as shown in Fig. 5(a).

The form of the last term in Eq. (15) is suggestive of a broadening mechanism involving paramagnetic spins in the matrix or at the surfaces of the particles. In Fig. 8 the temperature dependence of the linewidth according to Eq. (15) for 200 Å particles is shown as the solid curve. Points calculated from Eqs. (6), (7), and (9) and (10) for broadening in the cases of strong exchange coupling, weak exchange coupling, and dipolar interaction, respectively, are also shown in Fig. 8, with the various parameters associated with the localized spins chosen to given agreement between the points and the solid curve.

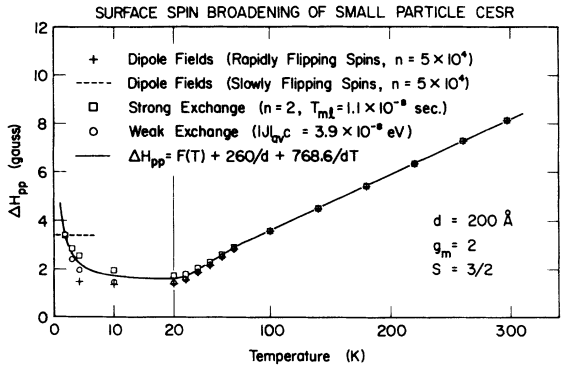

FIG. 8. Comparison of Eq. (15) (solid line) with points calculated from Eqs. (6), (7), and (9) and (10) representing strong exchange broadening, weak exchange broadening, and dipole field broadening respectively, for $d = 200$ Å. Surface spins with $g_m = 2$ and $S = \frac{3}{2}$ are assumed. Note scale change at $T = 20$ K.

1. Strong exchange coupling

Good agreement was obtained assuming two surface spins ($c \sim 20$ ppm), $g_m = 2$, $S = \frac{3}{2}$, and $T_{m1} = 1.1 \times 10^{-8}$ sec. These numbers are not unreasonable; the sample is known to contain, for example, approximately 7 ppm of potentially magnetic manganese atoms.

2. Weak exchange coupling

Good agreement was found for $|J|_{av} c = 3.9 \times 10^{-8}$ eV, $g_m = 2$, and $S = \frac{3}{2}$. For example, $|J|_{av} = 10^{-4}$ eV would require a concentration $c = 3.9 \times 10^{-3}$, or about 40 surface spins for a 200 Å particle. Such a concentration of spins would be consistent with the presence of high concentrations of N_2^- and other radiation damage centers in x-irradiated NaN_3.

3. Dipole field broadening

This possibility appears less viable. Even assuming a transition from rapidly to slowly flipping spins between 4.2 and 77 K, it is still necessary to have about 5×10^4 spins near each 200 Å particle. This constitutes several times the number of surface atoms of the particle.

We conclude that the low-temperature broadening may be accounted for by spins in the matrix, and if so, the spins must be in close enough proximity to the particle surfaces to interact with the conduction electrons via exchange.

For the mechanisms considered, the dependence of the low-temperature broadening on particle size depends on how the surface spin concentration varies with particle growth. Additional data are required to determine the accuracy of the inverse d dependence we have taken in the last term of Eq. (15).

B. Quantum size effect

Since the conduction-electron spin relaxation time for a small particle with discrete energy levels should be quite long, the use of very low microwave power levels may be necessary for detection of CESR. We have observed at very low power level in sample *SC*1 at 4.2 K a broad easily saturated signal [Fig. 5(b)] appearing at the sodium g value in superposition with the narrower resonance observed at higher power levels. We believe this broad line represents a hyperfine envelope of narrow lines resulting from level discreteness in the smallest particles in the sample. The saturability of this signal indicates that the conduction-electron spins are not being rapidly relaxed via an exchange interaction with surface spins; possibly, the broad resonance originates from those particles which have no adjacent surface spins. Attributing the 28 G linewidth of the broad resonance to contact hyperfine broadening, we find that Eq. (12) indicates a particle size of 24 Å. From Fig. 1 it is seen that Kawabata's theory[5] predicts a negligible linewidth and shift for 24 Å particles. We estimate that the integrated intensity of the broad line is at least twice that of the narrow one, which is consistent with the large enhancement in static susceptibility expected for 24 Å particles at 4.2 K due to level discreteness.[29]

It is necessary to point out a discrepancy between Eq. (12) and the data of Smithard.[14] For 20 Å particles Smithard reported a Lorentzian CESR line of width approximately 15.5 G at 77 K, while Eq. (12) would predict a Gaussian resonance of width 40 G. Maintaining consistency with Smithard's data, the hyperfine broadening has not been included in the analysis in Part A of this section. Smithard's failure to observe hyperfine broadening may have been because his particles were larger than his optical measurements indicated. Alternatively, it is conceivable that many of the Na particles in x-irradiated NaN_3 samples form in clusters (e.g., along dislocations) so that the interparticle separations are small enough for tunneling of electrons between particles to reduce the hyperfine broadening.

V. CONCLUSIONS

An interpretation has been presented of the results of CESR measurements on colloidal sodium particles in x-irradiated NaN_3, taking account of the following features of the data:

(i) variation in the slope of the linewidth vs temperature curve between 77 and 300 K among samples;

(ii) enhancement of the wings of the resonance line in a sample for which the linewidth vs temperature slope was large;

(iii) low-temperature broadening of the CESR line;

(iv) the appearance in sample *SC*1 of a broad, easily saturated resonance at the CESR g value of sodium at 4.2 K for very low microwave power level.

In our interpretation, features (i) and (ii) are the result of a broad particle size distribution, with appropriate relative weighting of large and small sizes; feature (iii) is associated with the presence of spins in the matrix in close proximity to particle surfaces; and feature (iv) is explained as the result of quantum level separation narrowing of CESR lines from the smallest particles in the sample combined with inhomogeneous broadening

from a distribution of contact hyperfine fields.

For sample *SC*1, in which all the above features were observed, we have deduced approximate expressions for the linewidth as a function of particle size [Eq. (15)], and for the particle size distribution (Fig. 7), although an accurate empirical expression for the CESR linewidth vs particle size awaits successful experimental determination of the particle size distributions.

Our principal conclusions may be summarized as follows:

(1) Low-temperature broadening of CESR lines in the small Na particles can be accounted for by the presence of spins in the matrix provided they are in close enough proximity to the particles to interact via exchange with the conduction electrons.

(2) It is necessary to use very low microwave power levels to observe quantum level separation CESR line narrowing in very small Na particles, and the width of the contact nuclear hyperfine evvelope of the resonance provides a means of estimating the particle size.

(3) Large values of the slope of linewidth vs temperature and enhancement of the wings of the resonance are associated with the presence of a broad particle size distribution.

The possibility that the broad resonance in Fig. 5(b) is associated with a paramagnetic center rather than with conduction electrons cannot be ruled out, but based on the g value and intensity, together with the observation that when the total line shape of Fig. 5(b) is resolved into a narrow and a broad component, the broad component is not of the form of a simple resonance line, it is likely that the broad line represents a manifestation of level discreteness in small sodium particles.

ACKNOWLEDGMENTS

The author is indebted to Professor W. D. Knight and Professor A. M. Portis for their interest and for many enlightening discussions. Dr. Melvin P. Klein kindly made available the Varian E-3 spectrometer. Thanks are also due to Dr. Philip Yee for edifying discussions about small particles, and to Dr. James P. Wolfe for advice concerning the superheterodyne spectrometer.

---

*Supported in part by the National Science Foundation; this work is based on the thesis of Daniel A. Gordon, submitted in partial satisfaction of the requirements for the Ph.D., University of California, 1975.

†Present address: Physics Department, Arizona State University, Tempe, Ariz. 85281.

[1]For example, G. Feher and A. F. Kip, Phys. Rev. 98, 337 (1955) (Li, Na, K, Be); W. M. Walsh, Jr., L. W. Rupp, Jr., and P. H. Schmidt, Phys. Rev. Lett. 16, 181 (1966) (Rb, Cs); J. H. Orchard-Webb and J. E. Cousins, Phys. Lett. A 28, 236 (1968) (Mg); L. Jannsens, A. Stesmans, J. Cousins, and J. Witters, Phys. Status Solidi B 67, 231 (1975) (Al); P. Damay, T. David, and M. J. Sienko, J. Chem. Phys. 61, 4369 (1974) (Ca).

[2]S. Schultz, in *Proceedings of the Fifteenth Colloque Ampere, Grenoble* (North Holland, Amsterdam, 1969), p. 108.

[3]R. Kubo, J. Phys. Soc. Jpn. 17, 975 (1962).

[4]B. W. Holland, in *Proceedings of the Fourteenth Colloque Ampere, Ljubljana* (North-Holland, Amsterdam, 1967), p. 468.

[5]A. Kawabata, J. Phys. Soc. Jpn. 29, 902 (1970).

[6]C. Taupin, J. Phys. Chem. Solids 28, 41 (1967); K. Saiki, T. Fujita, Y. Shimizu, S. Sakoh, and N. Wada, J. Phys. Soc. Jpn. 32, 447 (1972); J.-P. Borel, C. Borel-Narbel, and R. Monot, Helv. Phys. Acta 47, 537 (1975).

[7]R. C. McMillan, G. J. King, B. S. Miller, and F. F. Carlson, J. Phys. Chem. Solids 23, 1379 (1962); M. Smithard, Solid State Commun. 14, 411 (1974).

[8]R. C. McMillan, J. Phys. Chem. Solids 25, 773 (1964).

[9]J.-L. Millet and R. Monot, in *Proceedings of the Eighteenth Colloque Ampere, Nottingham* (North-Holland, Amsterdam, 1975), p. 319.

[10]R. Monot, C. Narbel, and J.-P. Borel, Nuovo Cimento B 19, 253 (1974).

[11]R. Dupree, C. T. Forwood, and M. J. A. Smith, Phys. Status Solidi 24, 525 (1967); R. Monot, A. Châtelain, and J.-P. Borel, Phys. Lett. A 34, 57 (1971).

[12]W. S. Glaunsinger and R. F. Marzke, Bull. Am. Phys. Soc. 20, 411 (1975).

[13]C. Taupin, J. Phys. Chem. Solids 28, 41 (1967).

[14]M. Smithard, Solid State Commun. 14, 407 (1974); 14, 411 (1974).

[15]F. J. Dyson, Phys. Rev. 98, 349 (1955). Our Eq. (5) differs from Dyson's result by a factor of 2 since Dyson defined ϵ as the probability of "spin disorientation" rather than spin reversal.

[16]V. N. Lisin and B. M. Khabibullin, Fiz. Tverd. Tela 17, 1045 (1975) [Sov. Phys.-Solid State 17, 1598 (1975)].

[17]A. R. Rodriguez and J. S. Helman (unpublished).

[18]M.B. Walker, Phys. Rev. B 3, 30 (1971).

[19]For example, J. H. Pifer and R. T. Longo, Phys. Rev. B 4, 3797 (1971); Phys. Rev. B 6, 2887 (1972).

[20]P. Monod and S. Schultz, Phys. Rev. 173, 645 (1968).

[21]G. E. Pake and T. L. Estle, *The Physical Principles of Electron Paramagnetic Resonance*, 2nd Ed. (Benjamin, Reading, Mass., 1973), p. 241.

[22]R. T. Schumacher and W. E. Vehse, J. Phys. Chem. Solids 24, 297 (1963).

[23]C. Kittel, *Introduction to Solid State Physics*, 4th ed. (Wiley, New York, 1966), p. 38.

[24]J. R. Asik, M. A. Ball, and C. P. Slichter, Phys. Rev. 181, 645 (1969); R. A. B. Devine and R. Dupree, Phys. Lett. A 30, 211 (1969).

[25]E. Gelerinter and R. H. Silsbee, J. Chem. Phys. 45, 1703 (1966).

[26]Y. Yafet, in *Solid State Physics*, edited by F. Seitz and D. Turnbull (Academic, New York, 1963), Vol. 14,

p. 1.
[27]Many of the numbers in this section, if viewed as measured values, have large uncertainties, so that the use of several significant digits appears unjustified. These significant digits are retained only to provide consistency among values chosen for the parameters of our model. These values are chosen to demonstrate that the model can give agreement with the data, and can be considered rough estimates of the true values.
[28]W. Kolbe, Phys. Rev. B 3, 320 (1971).
[29]R. Denton, B. Mühlschlegel, and D. J. Scalapino, Phys. Rev. B 7, 3589 (1973).